

# High-bandwidth viscoelastic properties of aging colloidal glasses and gels

S. Jabbari-Farouji<sup>1,2</sup>, M. Atakhorram<sup>3</sup>, D. Mizuno<sup>3,4</sup>, E. Eiser<sup>5,6</sup>,  
G.H. Wegdam<sup>1</sup>, F.C. MacKintosh<sup>3</sup>, Daniel Bonn<sup>1,7</sup>, C.F. Schmidt<sup>4,8</sup>

<sup>1</sup>*van der Waals-Zeeman Instituut, Universiteit van Amsterdam, 1018XE Amsterdam, The Netherlands*

<sup>2</sup>*Group Polymer Physics, Department of Applied Physics,*

*Technische Universiteit Eindhoven 5600MB Eindhoven, The Netherlands*

<sup>3</sup>*Divisie Natuur- en Sterrenkunde, Vrije Universiteit Amsterdam, 1081HV Amsterdam, The Netherlands*

<sup>4</sup>*Organization for the Promotion of Advanced Research,*

*Kyushu University, Higashi-ku, Hakozaki 6-10-1, 812-0054 Fukuoka, Japan*

<sup>5</sup>*van 't Hoff Institute for Molecular Sciences, Universiteit van Amsterdam, 1018WV Amsterdam, The Netherlands*

<sup>6</sup>*University of Cambridge, Department of Physics,*

*Cavendish Laboratory, J J Thomson Avenue, Cambridge CB3 0HE, UK*

<sup>7</sup>*Laboratoire de Physique Statistique de l'ENS, 75231 Paris Cedex 05, France*

<sup>8</sup>*Physikalisches Institut, Georg-August-Universitt, 37077 Göttingen, Germany*

(Dated: October 18, 2018)

We report measurements of the frequency-dependent shear moduli of aging colloidal systems that evolve from a purely low-viscosity liquid to a predominantly elastic glass or gel. Using microrheology, we measure the local complex shear modulus  $G^*(\omega)$  over a very wide range of frequencies (1 Hz- 100 kHz). The combined use of one- and two-particle microrheology allows us to differentiate between colloidal glasses and gels - the glass is homogenous, whereas the colloidal gel shows a considerable degree of heterogeneity on length scales larger than 0.5 micrometer. Despite this characteristic difference, both systems exhibit similar rheological behavior which evolve in time with aging, showing a crossover from a single power-law frequency dependence of the viscoelastic modulus to a sum of two power laws. The crossover occurs at a time  $t_0$ , which defines a mechanical transition point. We found that the data acquired during the aging of different samples can be collapsed onto a single master curve by scaling the aging time with  $t_0$ . This raises questions about the prior interpretation of two power laws in terms of a superposition of an elastic network embedded in a viscoelastic background. *keywords: Aging, colloidal glass, passive microrheology*

PACS numbers:

## I. INTRODUCTION

Soft glassy materials are ubiquitous in everyday life. A common feature of all such materials is their relatively large response to small forces (hence soft) and their disordered (glassy) nature. Pertinent examples of such systems are foams, gels, slurries, concentrated polymer solutions and colloidal suspensions. These systems show interesting viscoelastic properties; depending on the frequency with which they are perturbed, they can behave either liquid- or solid-like. In spite of their importance for numerous applications, the mechanical behavior of such soft glassy materials is still incompletely understood [1].

In recent decades, colloidal suspensions have been used extensively as model systems for the glass transition in simple liquids [2, 3, 4] and gel formation [5]; since the diffusion of the particles can easily be measured using, e.g., light scattering or confocal microscopy [6]. The viscoelasticity of such systems, especially its development during the aging of glassy systems or the formation of a gel, has, however, received relatively little attention.

Another issue that deserves attention is differentiating between colloidal gels and glasses in terms of their rheological properties [7]. The main difference between colloidal gels and glasses stems from their structure. While the glass has a homogenous liquid-like structure with no long-range order, a gel can have a heterogeneous struc-

ture whose characteristic length is set by the mesh size of the gel network (see Fig. 1) [12].

As an example of a soft glassy system, we here focus on the viscoelasticity of Laponite suspensions for which a very rich phase diagram has been reported [8, 9]. When dissolved in water, Laponite suspensions evolve from a liquid-like state to a non-ergodic solid-like state [3, 4, 10, 11]. During this process the mobility of the particles slows down and viscoelasticity develops. This system is an interesting one to study since both colloidal gels and glasses can be obtained depending on Laponite concentration and added salt content [12]. Therefore, it provides us with the possibility to investigate the similarities and differences in the viscoelastic properties of the two types of non-equilibrium states.

To study the mechanical properties of gels and glasses, we used microrheology (MR), which allows us to measure frequency-dependent shear moduli over a wide range of frequencies. This technique is based on the detection of small displacements of probe particles embedded in the soft glassy material, from which we obtain the mechanical properties of surrounding matrix [21]. Considering the fragility of soft materials, this technique is ideally suited for our studies, since it is less invasive than conventional rheometry.

Here we have used a combination of one and two-particle MR Measurements [15, 24] to probe the mechan-

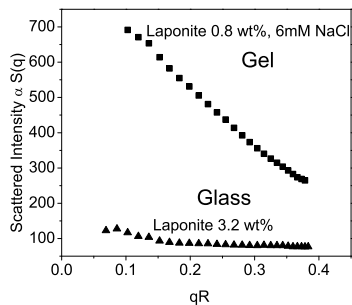


FIG. 1: Light scattering intensity relative reduced with respect to scattered intensity from toluene for two samples a) Laponite 3.2 wt% and b) Laponite 0.8 wt%, 6 mM NaCl. The data points are taken at late stages of aging when the scattering intensity has stabilized.

ical properties and possible inhomogeneities of colloidal gels and glasses on length scales of the order of the particle size  $1\mu\text{m}$  and separation distances of the order of  $5\text{-}20\mu\text{m}$ .

## II. EXPERIMENTAL

### A. Materials

We have studied charged colloidal disks of Laponite XLG, with an average radius of  $15\text{ nm}$  and a thickness of  $1\text{ nm}$ . Laponite can absorb water, increasing its weight up to  $20\%$ . Therefore, we first dried it in an oven at  $100^\circ\text{C}$  for one week and subsequently stored it in a desiccator.

We prepared a number of Laponite samples with different concentrations and salt contents. Laponite solutions without added salt were prepared in ultra pure Millipore water ( $18.2\text{ M}\Omega\text{ cm}^{-1}$ ) and were stirred vigorously with a magnet for  $1.5\text{ hours}$  to make sure that the Laponite particles were fully dispersed. The dispersions were filtered using Millipore Millex AA  $0.8\mu\text{m}$  filter units to obtain a reproducible initial state [4]. This instant defined the zero of waiting time,  $t_w = 0$ .

The Laponite solutions with  $\text{pH}=10$  were obtained by mixing the Laponite with a  $10^{-4}$  mole/l solution of NaOH in Millipore water. The samples with non-zero salt content were prepared by diluting the Laponite suspensions in pure water with a more concentrated salt solution [13]. For instance, a sample of  $0.8\text{ wt}\%$ ,  $6\text{mM NaCl}$  was prepared by mixing equal volumes of  $1.6\text{ wt}\%$  Laponite solution in pure water with a  $12\text{mM}$  salt solution.

For the microrheology measurements, we added a small fraction, below  $10^{-4}$  vol %, of silica beads with a diameter of  $1.16\mu\text{m} \pm 5\%$  [14] immediately after the preparation of the sample. Subsequently we infused the solution into a sample chamber of about  $50\mu\text{l}$  volume, consisting of a coverslip and microscope slide separated by spacers of double-sided tape with a thickness of  $70\mu\text{m}$ , sealed with vacuum grease at the ends to avoid evaporation

of the sample. All the experiments were performed at room temperature ( $21 \pm 1^\circ\text{C}$ ). After placing the sample chamber into the microscope, we trapped two beads and moved them to about  $20\mu\text{m}$  above the bottom glass surface.

### B. Microrheology

The experimental setup for performing one- and two-particle MR consists of two optical tweezers formed by two independent, polarized laser beams  $\lambda_1 = 1064\text{ nm}$  (Nd:YVO4, CW) and  $\lambda_2 = 830\text{ nm}$  (diode laser, CW) which can trap two particles at a variable separation  $r$ . Details of the experimental setup can be found in [15, 16]. Stable trapping is achieved using a high numerical aperture objective lens which is part of a custom-built inverted microscope. Two lenses in a telescope configuration allow us to control of the position of the beam foci in the plane perpendicular to the beam directions. The two beams are focused into the sample chamber through a high numerical objective of the microscope ( $100\times$ , NA 1.3).

Back-focal-plane interferometry is used to measure the position fluctuations of the probe bead away from the trap center [17]. The signals emerging from each of the traps are separately projected onto two independent quadrant photodiodes, yielding a spatial resolution for the particle position that is better than  $1\text{ nm}$ .

During our measurements, the power of each laser was typically less than  $10\text{ mW}$ . Labview software was used to acquire time series data of particle positions from the QPDs for a minimum time of  $45\text{ s}$ . The data were digitized with an A/D converter at  $195\text{ kHz}$  sampling rate.

### C. Macrorheology

The viscoelastic moduli during the aging process were also measured using a conventional Anton Paar Physica MCR300 rheometer in Couette geometry. To avoid perturbing the sample during the aging process we performed the oscillatory shear measurements with a strain amplitude of  $0.01$  in the frequency range of  $0.1\text{-}10\text{ Hz}$ . In order to prevent evaporation during the long time measurements, we installed a vapor trap.

### D. Light scattering

Our light scattering setup (ALV) is based on a He-Ne laser ( $\lambda = 632.8\text{ nm}$ ,  $35\text{ mW}$ ) and avalanche photodiodes as detectors. Static light scattering experiments were performed (scattering angle range  $20\text{-}150^\circ$  on non-ergodic samples at late stages of aging when the scattered intensity had stabilized. Samples were rotated to average over different positions in the sample.

### III. THEORY AND DATA ANALYSIS

There are two classes of microrheology (MR) techniques: active (AMR) and passive (PMR) [18]. In the first of these, the response of a probe particle to a calibrated force is measured. In the second approach, only passive, thermal fluctuations are monitored, from which one can infer the response function and the rheological properties of the surrounding medium using the fluctuation-dissipation theorem (FDT). Applying the FDT assumes thermal equilibrium. It may therefore be potentially problematic to apply PMR to such non-equilibrium systems as aging glasses. Nevertheless, in a prior study [19], we not only directly confirmed the validity of the FDT, but also found excellent agreement between active and passive methods in the slowly aging Laponite glass. Therefore, in what follows we will use only the passive method, which has the significant advantage that, with a single measurement of the fluctuation power spectrum, one can determine the complex shear modulus simultaneously over a wide range of frequencies [20, 21, 22, 23].

#### A. One-particle Microrheology

In one-particle MR, we first extract the complex compliance from the position fluctuations of one particle. The time-series data of the bead displacement measured by the quadrant photodiode is Fourier transformed to calculate the power spectral density of displacement fluctuations:

$$\langle |x(\omega)|^2 \rangle = \int_{-\infty}^{\infty} \langle x(t)x(0) \rangle e^{i\omega t} dt \quad (1)$$

This is done for  $x$  and  $y$  directions in the plane normal to the laser beam. The power spectral density of the thermal fluctuations of the probe is related to the imaginary part of the complex compliance  $\alpha(\omega) = \alpha'(\omega) + i\alpha''(\omega)$  via the FDT:

$$\alpha''(\omega) = \frac{\omega \langle |x(\omega)|^2 \rangle}{2k_B T}. \quad (2)$$

Provided that  $\alpha''(\omega)$  is known over a large enough range of frequencies, one can recover the real part of the response function from a Kramers-Kronig (principal value) integral:

$$\alpha'(\omega) = \frac{2}{\pi} P \int_0^{\infty} \frac{\omega' \alpha''(\omega')}{\omega'^2 - \omega^2} d\omega'. \quad (3)$$

Before calculating the shear modulus from the response function, we calibrate the setup and correct for the trap stiffness that shows up at low frequencies as explained in detail in [17, 24].

The complex shear modulus  $G^*(\omega) = G'(\omega) + iG''(\omega)$  can be obtained from the corrected complex compliance

through the generalized Stokes relation, valid for incompressible and homogenous viscoelastic materials [20, 21]

$$G^*(\omega) = \frac{1}{6\pi R \alpha(\omega)}, \quad (4)$$

where  $R$  is the radius of the probe bead.

#### B. Two-particle microrheology

In two-particle MR, we calculate the correlated fluctuations of two probe beads inside the material. Such measurements probe the viscoelastic properties of the medium on length scales comparable to the interparticle separation. In general, with more than one probe particle, the displacement of particle  $m$  in direction  $i$  is related to the force applied to particle  $n$  in direction  $j$  via the complex response tensor  $u_i^{(m)}(\omega) = \alpha_{ij}^{(m,n)}(\omega) F_j^{(n)}(\omega)$ . In the case of two particles, the response tensors  $\alpha_{ij}^{(1,1)}$  and  $\alpha_{ij}^{(2,2)}$  describe how each of the particles 1 and 2 respond to the forces applied to the particle itself, while  $\alpha_{ij}^{(1,2)}$  describes how particle 1 responds to the forces on particle 2.

In thermal equilibrium and in the absence of external forces, the FDT again relates the imaginary part of the response tensor to the spectrum of displacement fluctuations of the particles.

$$\alpha_{ij}^{(m,n)}(\omega) = \frac{\omega}{2k_B T} S_{ij}^{(m,n)}(\omega), \quad (5)$$

where the spectra of thermal fluctuations  $S_{ij}^{(m,n)}$  are defined as

$$S_{ij}^{(m,n)}(\omega) = \int_{-\infty}^{\infty} \langle u_i^{(m)}(t) u_j^{(n)}(0) \rangle e^{i\omega t} dt. \quad (6)$$

The problem of two hydrodynamically correlated particles in a viscoelastic medium and the relation between the response tensor and the rheological properties of the medium has been worked out in [25]. The self-parts of response tensor  $\alpha_{ii}^{(1,2)}$  are the same as the ones obtained from one-particle microrheology.

The cross component part of the response tensor  $\alpha_{ij}^{(1,2)}$  can be decomposed into two parts  $\alpha_{\parallel}$  parallel to the vector  $\mathbf{r}$  separating the two beads and  $\alpha_{\perp}$  perpendicular to  $\mathbf{r}$ :  $\alpha_{ij}^{(1,2)} = \alpha_{\parallel} \hat{r}_i \hat{r}_j + \alpha_{\perp} (\delta_{ij} - \hat{r}_i \hat{r}_j)$ . For incompressible fluids each of the components are related to the complex shear modulus via a generalization of the Oseen tensor:

$$\alpha_{\parallel}(\omega) = 2\alpha_{\perp}(\omega) = \frac{1}{4\pi r G^*(\omega)}. \quad (7)$$

Similarly to the one-particle method, the measured response function must be corrected for the trap stiffness. The trap correction for two-particle microrheology has been explained in detail in reference [24].

#### IV. RESULTS

We carried out the measurements on a variety of Laponite concentrations and salt contents (2.8, 3.2 wt%, in pure water, 3 wt% in pH=10, 1.5 wt %, 5mM NaCl, 0.8 wt %, 6mM NaCl, 0.8 wt %, 3mM NaCl ). We have chosen these samples to ensure that their rate of aging is slow enough to guarantee that no significant aging occurs during each measurement. On the other hand they evolve fast enough to allow us to follow the whole evolution within a few hours. The samples 2.8, 3.2 wt%, in pure water, 3 wt% in pH=10 and 1.5 wt %, 5mM NaCl showed the properties of a glassy sample according to our light scattering data and samples 0.8 wt %, 6mM NaCl, 0.8 wt %, 3mM NaCl behaved like a colloidal gel [26, 27]. In addition, we find that a pH of 10 did not affect the aging dynamics qualitatively. It merely acted as an electrolyte that slightly accelerated the aging. The same held for Laponite 1.5 wt%, 5mM NaCl. In this case salt just accelerated the aging, but it did not change the underlying dynamics of the aging process. As we demonstrated elsewhere [26] both samples belong to the glass region of the phase diagram.

For the detailed discussion of our results, we focus on two samples that are representative of the others: one sample that behaves as a glass ( $C=3.2$  wt%), and one sample ( $C=0.8$  wt%, 6mM NaCl) that behaves like a gel. In the latter case, the structure factor shows a strong  $q$ -dependence, as illustrated in Fig. 1. This suggests a more heterogenous, gel-like structure, in contrast to the more homogenous samples that we identify as a glass. In the following, we shall characterize our samples as gels or glasses in this way.

To follow the aging of the systems we trapped a bead in a single laser trap and measured the displacement power spectral densities (PSD) as a function of waiting time. Since the system evolves towards a non-ergodic state, the time average may not necessarily be equal to the ensemble average for the measured PSDs. However, in our range of frequencies ( $1 - 10^5$  Hz) we confirmed that our results did not depend on the time interval used to compute the time average. Thus, we can use the time-averaged PSD without averaging over several beads in our study.

Fig. 2 shows the measured displacement PSDs as a function of frequency during the aging of the glass and the gel respectively. We normalized the PSDs with the diffusion coefficient ( $D_0 = kT/(6\pi\eta_{water}R_{bead})$ ) of a same-size bead measured in water, so that the normalized PSDs will be independent of bead size. It is evident that in both systems the particle motion progressively slows down with increasing aging time  $t_w$ , reflecting the increase of viscosity in the system. The PSDs in both samples start from a state close to water, for which  $\langle |x(\omega)|^2 \rangle / 2D_0 = 1/\omega^2$ . Gradually their amplitudes as well as the absolute values of their power-law slopes decrease with time. There is a crossover time  $t_0$  such that for  $t_w < t_0$ , the PSDs can be described by a single power

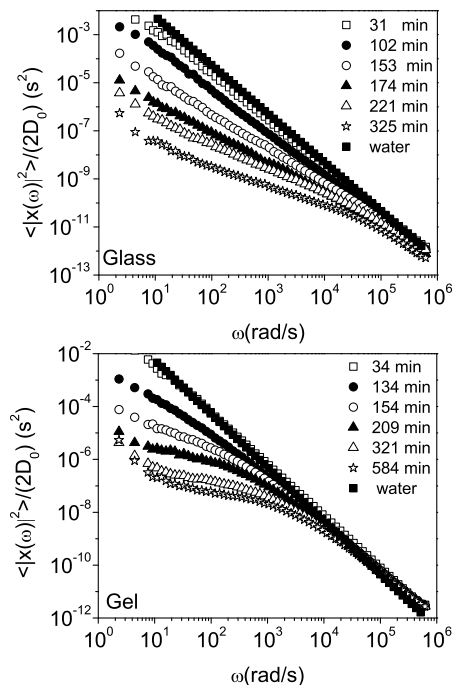


FIG. 2: Normalized displacement power spectral densities ( $\langle |x(\omega)|^2 \rangle / 2D_0$ ) of silica probe particles in a glassy sample (3.2 wt%, bead diameter  $1.16 \mu\text{m}$ ) and a gel-like sample (0.8 wt%, 6mM NaCl, bead diameter  $0.5 \mu\text{m}$ ) in the  $x$  direction) with increasing age after preparing the sample. Waiting times are given in the legend. The filled squares show the PSD of a bead in pure water for comparison. All experiments were done at  $21^\circ\text{C}$ .

law. At longer aging times  $t_w > t_0$ , two distinct slopes appear in the log-log plots (Fig. 2).

The evolution of the local shear moduli  $G^*$  obtained from PSDs are shown in Fig. 3 (glass) and 4 (gel). The shear moduli are derived from single particle MR according to Eq. (4). It is evident that the systems evolve from an initially completely viscous to a strongly viscoelastic fluid. At the early stages of aging, the loss modulus is still much larger than the storage modulus ( $G'' \gg G'$ ) representing a more liquid-like state. With time the samples become more solid-like: the elastic modulus becomes larger than the loss modulus ( $G'' \ll G'$ ). We observe also that the changes in  $G'$  are more dramatic than the changes in  $G''$ . While  $G''$  almost saturated after 170 min for the glass and 100 min for the gel,  $G'$  continues to grow with time.

Visual inspection showed that the gel was “softer” than the glass. When we mechanically shook similar tubes containing gel or glass, the gel liquefied at a clearly smaller stress: it appears that gels had a lower yield stress compared to glasses. Therefore it is reasonable to expect that gels also have a lower viscoelastic modulus than glasses, as comparison of Fig. 3 and Fig. 4 indeed confirms. Furthermore, the ratio  $G'/G''$  at low frequencies is higher in the gel ( $G'/G'' = 30$  for Laponite

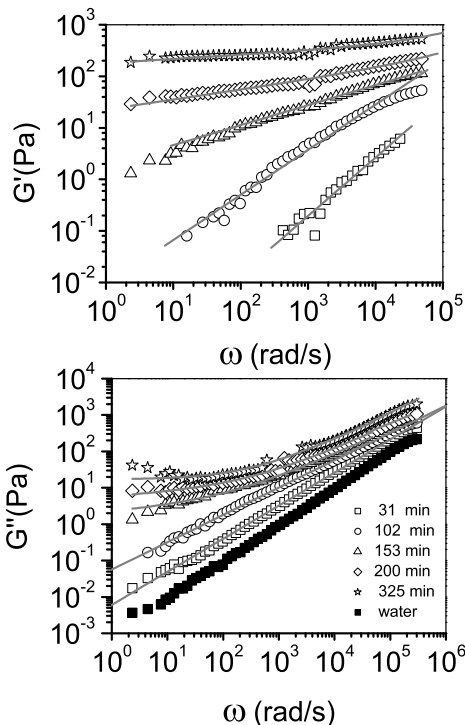


FIG. 3: Glass data: The symbols show the shear moduli  $G'(\omega)$  and  $G''(\omega)$  (absolute magnitude) as a function of frequency measured using  $1.16 \mu\text{m}$  silica probe particles in a 3.2 wt% Laponite solution in pure water with increasing aging time after preparing the sample. Aging times are given in the legend. The lines show the fits of  $G'(\omega)$  and  $G''(\omega)$  according to  $C_1(-i\omega)^a + C_2(-i\omega)^b$  in which  $C_2 = 0$  for aging times  $t_w < 120$  min.

0.8 wt%, 6mM) compared to the glass ( $G'/G'' = 12$  for Laponite 0.8 wt%), at late stages of aging when  $G''$  has almost saturated and  $G'$  evolves very slowly.

From microrheology we conclude that the aging behaviors of gels and glasses are qualitatively similar. We know, however, from light scattering measurements that the underlying structures of gels and glasses are very different [12]. Since spatial heterogeneity is the defining feature of gels, we thus set out to investigate if local measurements of microrheology across the samples can detect the difference between gels and glasses.

### A. Heterogeneity

Heterogeneities within a sample can be explored by measuring the PSDs of multiple beads at different positions in the sample. A discrepancy between the shear moduli obtained from one- and two-particle MR can also be used as an indicator of a heterogeneous structure. A further test of heterogeneity in a material is provided by comparison of MR with bulk rheology, as will be discussed below. To investigate the homogeneity of colloidal

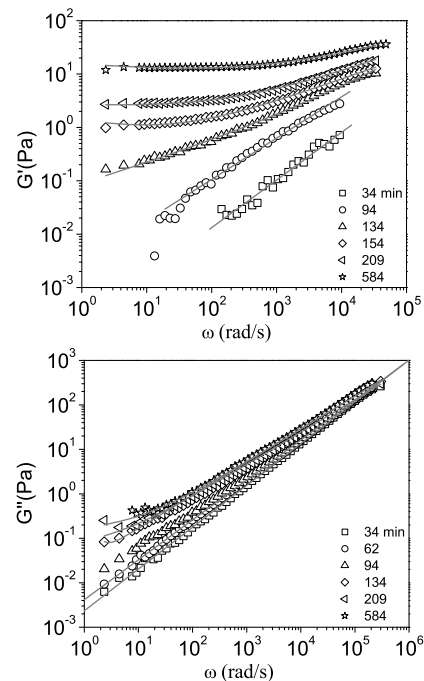


FIG. 4: Gel data: The symbols show the shear moduli  $G'(\omega)$  and  $G''(\omega)$  (absolute magnitude) as a function of frequency measured using a  $0.5 \mu\text{m}$  silica probe particle in a 0.8 wt% Laponite solution in 6 mM NaCl water with increasing aging time after preparing the sample. Aging times are given in the legend. The lines show the fits of  $G'(\omega)$  and  $G''(\omega)$  according to  $C_1(-i\omega)^a + C_2(-i\omega)^b$  in which  $C_2 = 0$  for aging times  $t_w < 100$  min.

gels and glasses of Laponite, we performed two types of measurement. First, we made simultaneous measurements of PSDs of two independent beads in two independent traps at different stages of aging. In another set of experiments, we measured PSDs of multiple beads in aged gels and glasses. The results of our experiments for both gels and glasses will be discussed below.

#### 1. Glass

For the glassy samples the displacement PSDs turned out to be independent of the bead position, as was concluded from a comparison of simultaneous measurements of PSDs of two independent beads in two independent traps during aging. Furthermore, the comparison between one- and two-particle MR reveals that within the experimental error, the complex shear moduli are identical to within the experimental error between the two methods for all stages of aging as shown in Fig. 5.

This was further verified by measuring the PSDs of several beads at different positions of an aged sample. As can be seen in Fig. 7, the measured shear moduli were independent of the position of the bead in the sample, verifying the homogeneity of the glassy sample, as shown

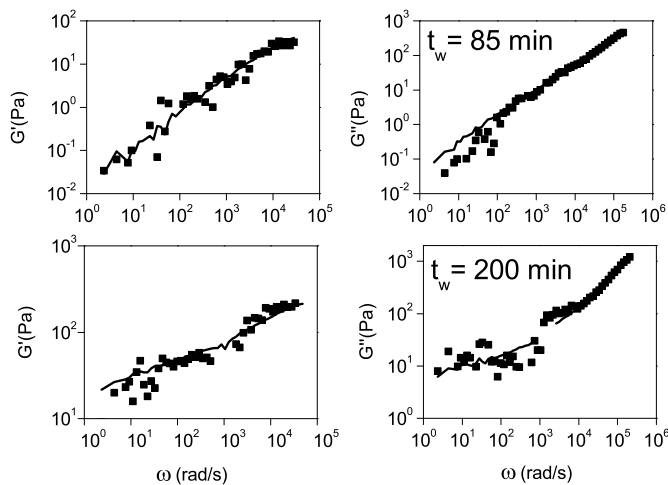


FIG. 5: Glass data: The shear moduli  $G'(\omega)$  and  $G''(\omega)$  (magnitude) at two different stages of aging in a 3.2 wt% Laponite solution derived from one- (lines) and two-particle (symbols) MR using  $1.16 \mu\text{m}$  silica probe particles. The distance between the two particles was  $6 \mu\text{m}$ . The aging times are shown in the figure. Note that in the late stages of aging the material becomes too stiff to obtain a good cross-correlation signal between the two beads over the background noise.

also in Fig. 6a.

These results suggest that the Laponite glass has a homogenous viscoelasticity, at least on length scales larger than half a micrometer, which is the length scale one-particle MR intrinsically averages over. An additional check on this can be obtained from a comparison between microrheology and macrorheology which should yield the same results if the sample is homogeneous.

Figure 8 shows the shear moduli extracted from MR and macrorheology experiments at a fixed frequency of ( $f = 0.7 \text{ Hz}$ ) during the course of aging. The overall agreement between macrorheology and MR is good. For the early stages of aging, the  $G''$  measured by the macrorheometer appears slightly higher, but this can be attributed to the large moment of inertia of the rheometer bob; macrorheology does not provide accurate measurements of the shear moduli when  $G^* < 1 \text{ Pa}$ . MR, on the other hand, has other sources of errors at low frequencies, especially for the late stages of aging, when the material becomes very rigid. In this case, the signal detected by the photodiode becomes small compared to the noise level;  $1/f$  laser pointing noise dominates at low frequencies. This is the most plausible explanation for the slight discrepancy between the results from the two methods at long aging times.

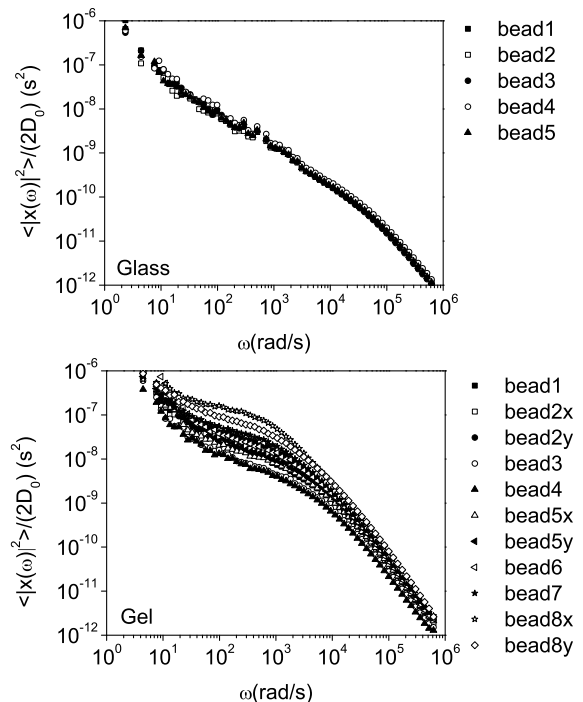


FIG. 6: The displacement PSDs of  $0.5 \mu\text{m}$  silica beads measured at different positions within an aged glass (Laponite 3.2 wt % in pure water,  $t_w \approx 5 \text{ h}$ ) and within an aged colloidal gel (Laponite 0.8 wt% in 6mM NaCl solution,  $t_w \approx 10 \text{ h}$ ).

## 2. Gel

Measuring the displacement PSDs of several beads at different positions of a gel at the late stages of aging revealed a considerable degree of inhomogeneity (Fig. 6). Not only were the PSDs position dependent, but at some positions in the sample the measured PSDs were also anisotropic, i.e. fluctuations in  $x$  and in  $y$  direction gave different results.

This result is consistent with the static light scattering measurements for this sample shown in Fig. 1 that suggest inhomogeneities of the gel on a length scale comparable to the inverse scattering vector, i.e. micrometers. Therefore, exploring such a gel using microrheology with a probe on the order of the mesh size of the network, one can detect these characteristic inhomogeneities. In (Fig. 9) we have plotted the shear moduli seen by the beads at different positions. It can be seen that there was an order of magnitude difference between the smallest and largest elastic moduli measured in the same sample and at the same time.

It is intriguing to ask when the heterogeneity starts to develop in the aging samples. It is likely to appear as a network-like structure is building up in the gel. To answer this question, we measured the PSDs of two beads at different positions of a gel as a function of aging time. We performed two sets of experiments: in the first one the

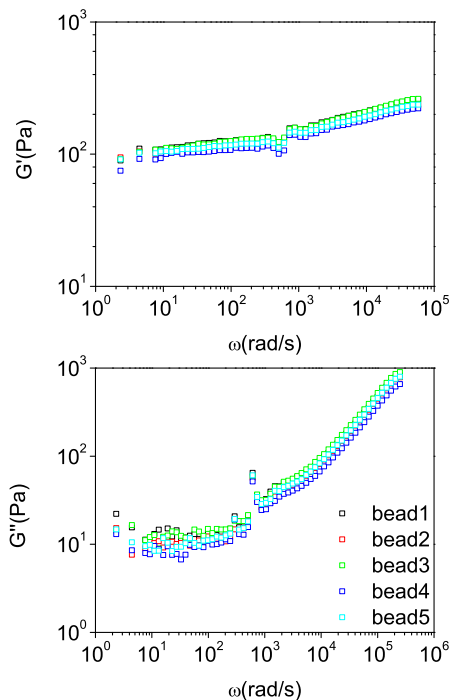


FIG. 7: Local elastic modulus  $G'$  and loss modulus  $G''$  measured at different positions in an aged glassy sample of Laponite 3.2 wt % in pure water ( $t_w \approx 5$ h)

two beads were positioned at a relatively close distance  $r = 4.66 \mu\text{m}$  (Fig. 10) and in the other one at a large distance of  $r = 19 \mu\text{m}$ .

In both experiments, the responses, i.e. the PSDs at different positions were equal in the early stages of aging. However, as time progressed, the PSDs measured at different positions began to differ. In addition, at later stages of aging, the displacement PSDs measured for some of the beads became anisotropic, meaning that the PSDs in the  $x$  and  $y$  directions were not equal anymore. In some measurements the anisotropy survived the latest measurement. For some other measurements, the anisotropy disappeared after some time (look at Fig. 10 for example). This suggests that the building up of structure in the gel is a dynamic process; at some points and times more particles join to the network and at some other points and times some particles disintegrate from the network.

Furthermore, our experiments showed that immediately after preparation, shear moduli obtained from two-particle MR and one-particle MR were equal. But already at relatively early stages of aging, the two-particle MR results differed from 1PMR results as demonstrated in Fig. 10. This deviation appeared long before the local shear moduli of the two beads in one-particle MR started to differ. For more details, see also [27].

Our measurements on several bead pairs at varying distances suggest that these inhomogeneities extend over a range of at least 100 micrometers. Therefore the macroscopic bulk shear modulus is not necessarily expected to

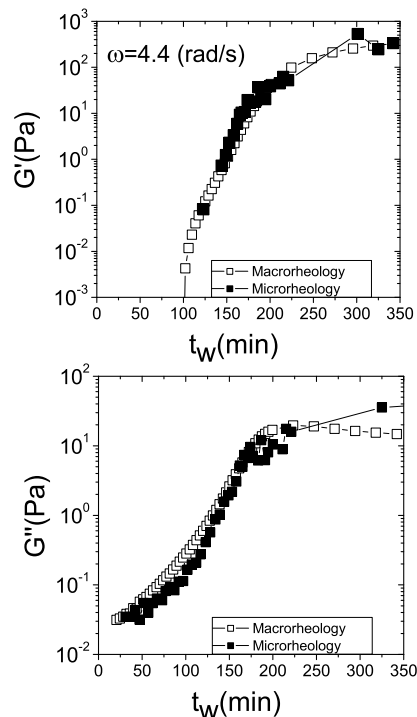


FIG. 8: Elastic and loss modulus as a function of aging time for a sample of Laponite 3.2 wt % in pure water obtained from macrorheology and one-particle MR at  $f = 0.7$  Hz. The strain amplitude in the macrorheology measurements was 0.01.

be equal to that measured by single particle MR. In Fig. 11, we compare the shear moduli obtained from one- and two-particle MR with the results of macrorheology at late stages of aging ( $t_w \approx 8.5$  h) when the changes in the loss and elastic moduli are slow. It is evident that the local shear modulus measured at one of the positions in the sample was equal to the bulk value, while the others reported a considerably lower shear modulus. Notably, the shear modulus obtained from the cross correlation of two-particles is lower than both bulk and local shear moduli. This suggests that two-particle MR can be used to detect inhomogeneities as long as they occur on length scales below the distance between the particles, but the results may still not reflect bulk properties if heterogeneities extend beyond the scale of the inter-particle distance.

## B. Model for the viscoelastic behavior

It has been noted in the context of weakly attractive colloids [28] and biopolymer networks [29] that the addition of two power law contributions describes the shear modulus very well. This result appears to reflect the existence of two distinct contributions to the viscoelasticity of the system and can be interpreted as a superposition of a more elastically rigid network (weakly frequency-dependent) and viscoelastic background (with a strong

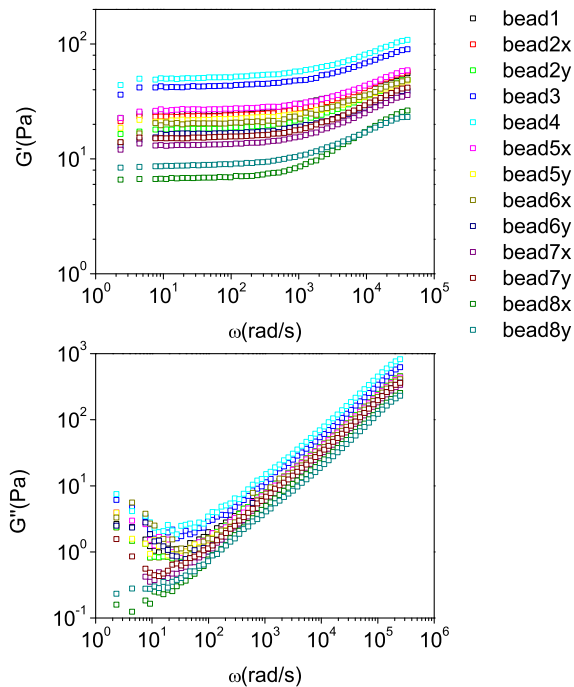


FIG. 9: Gel data: local elastic modulus  $G'$  and loss modulus  $G''$  measured at different positions in an aged gel sample of Laponite 0.8 wt % in 6mM NaCl solution ( $t_w \approx 10$ h)

frequency dependence).

Our data ( Fig. 3 and Fig. 4) can be interpreted in a similar manner: In addition to a strongly frequency-dependent viscoelastic response at high frequencies, a more elastic (weakly frequency-dependent) response appears after some aging time  $t_0$  and slowly increases in amplitude during the aging process. To be more precise, we see that the complex shear modulus of both gels and glasses crosses over from a single power law to a superposition of two power laws around a certain waiting time  $t_0$  which depends on the sample ( $t_0 \approx 155$ min for the glass sample of Laponite 3.2 wt % and  $t_0 \approx 95$ min for the gel sample of Laponite 0.8 wt %, 6mM NaCl ) [19]. The local shear moduli of both samples turn out to be well-described by the following expression:

$$G(\omega) = G'(\omega) + iG''(\omega) \equiv \begin{cases} C_1(-i\omega)^a & : t_w < t_0 \\ C_1(-i\omega)^a + C_2(-i\omega)^b & : t_w > t_0 \end{cases} \quad (8)$$

Physically, this model implies that two distinct stresses arise under a common imposed strain — in the way forces add for springs in parallel, as opposed to displacements/compliances that would add for springs in series. This response would be expected, for instance, for two interpenetrating structures/systems that displace together under strain, at least on the scale of our probe particles, which are large compared to the individual Laponite particles. This can, in principle, be the case whether or not the material appears to be homogeneous on this scale.

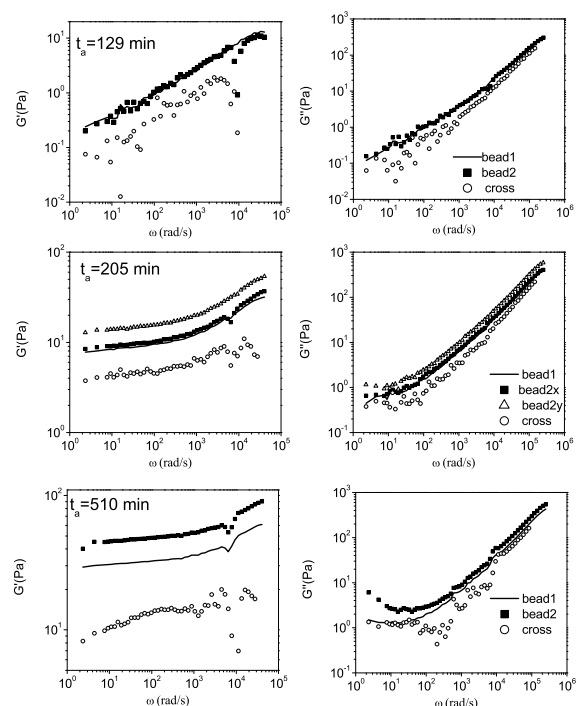


FIG. 10: Gel data: The shear moduli  $G'(\omega)$  and  $G''(\omega)$  at different stages of aging derived from one- and two-particle MR of  $0.5 \mu\text{m}$  silica probe particles in a gel of Laponite 0.8 wt % in 6mM NaCl solution. The distance between the two beads was  $4.66 \mu\text{m}$ . For  $t_a = 129$  min the shear moduli at two different positions are equal. At  $t_a = 205$  min the shear moduli at the two positions are not equal. Furthermore shear modulus at position 2 shows anisotropy. At a later time  $t_a = 510$  min the shear moduli at the two positions are not equal but the anisotropy observed earlier at position of bead 2 has been disappeared.

A tenuous elastic network structure immersed in a more fluid-like background, such as we might expect for a gel, would behave in this way, provided that the network and the background medium are strongly coupled hydrodynamically, and that the network spans length scales corresponding to the imposed strain. Such a gel could appear to be either homogenous or heterogeneous, depending on the length scale probed.

We find that the exponent of the single power law decreased from 1 to a value of about 0.7 before the second component becomes visible. The exponent and amplitude of the first component  $C_1(-i\omega)^a$  do not change further with aging time for  $t_w > t_0$  while the amplitude of the other one  $C_2$  grows appreciably over the same times.

In Fig. 12(a) and (c), we have plotted the evolution of the fitting parameters as a function of aging time for different samples. As can be seen in the figure, the development of the two viscoelastic components for different samples is qualitatively similar, although the rate of change depends on sample concentration and salt content.

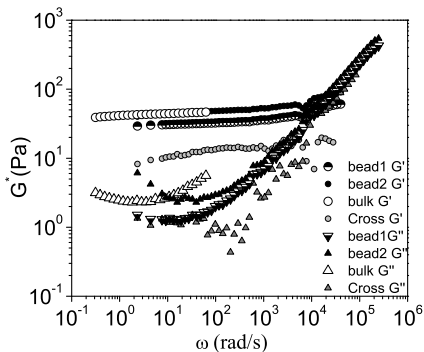


FIG. 11: Complex shear modulus at a late stage of aging  $t_w \approx 8.5$ h obtained from single-particle MR at two different positions of the sample, two-particle MR and bulk rheology in a sample of Laponite 0.8 wt%, 6mM NaCl. The circles show  $G'$  and triangles show  $G''$  values.

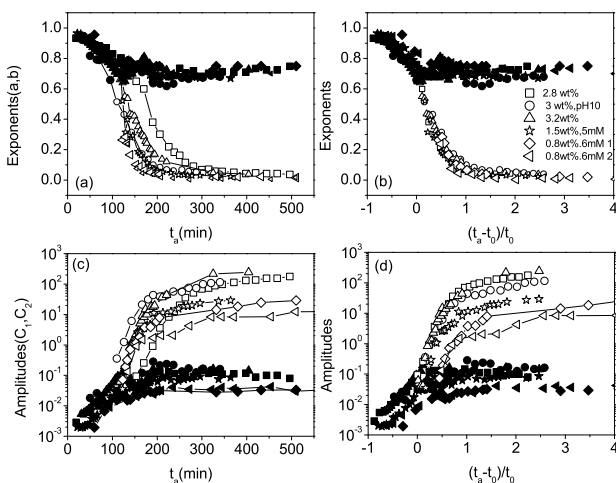


FIG. 12: The complex shear moduli of Laponite suspensions can be described as the sum of two power laws  $C_1(-i\omega)^a + C_2(-i\omega)^b$  in which  $C_2 = 0$  for waiting times  $t_w < t_0$ . The crossover times are  $t_0 = 155, 95, 120, 105, 95$  min for Laponite concentrations 2.8 wt%, 3 wt%, pH10, 3.2 wt%, 1.5 wt%, 5mM NaCl and two different positions of 0.8 wt%, 6mM NaCl, respectively. (a) The evolution of power-law exponents  $a$  (filled symbols) and  $b$  (open symbols) as a function of aging time for different concentrations of Laponite. (b) The exponents  $a$  (filled symbols) and  $b$  (empty symbols) as a function of scaled aging time (c) The amplitude of viscoelastic contributions  $C_1$  (filled symbols) and  $C_2$  (open symbols) as a function of aging for different samples. (d) The same as panel (c) but plotted versus scaled aging time. The sample concentrations are shown in the legend.

Interestingly, the evolution curves of the exponents  $a$  and  $b$  for the different samples superimpose if we scale the aging time as  $t'_a = (t_w - t_0)/t_0$ . The crossover times are  $t_0 = 155, 95, 120, 105, 95$  min for Laponite concentrations 2.8 wt%, 3 wt%, pH10, 3.2 wt%, 1.5 wt%, 5mM and 0.8 wt%, 6mM NaCl, respectively. For the amplitudes on the other hand, the data do not collapse. Especially the

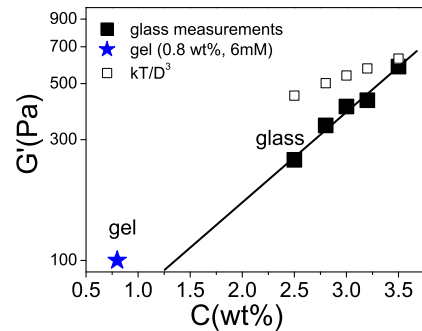


FIG. 13: Bold symbols: The elastic modulus obtained from macrorheology at late stages of aging at the aging time that there is a crossover to a fast regime of aging to a slower regime as a function of concentration measured for different glassy samples and a gel sample of 0.8 wt%, with 6mM salt at  $f = 0.05$  Hz. Empty symbols: An estimate of the plateau value  $G'_p \propto kT/D^3$  is shown for comparison.

amplitudes of the second (viscoelastic) component systematically decreases as the Laponite content is reduced. Furthermore, for the gel the amplitude depends on the position and we can see some fluctuations in the amplitude of the second component  $C_2$ , at later stages of evolution. This can be understood in terms of the dynamic process of gel formation in which Laponite particles still can join or detach from the network.

## V. DISCUSSION AND CONCLUSION

We have studied the evolution of the viscoelastic properties of a variety of Laponite suspensions including both gel-like and glassy states over a wide range of frequencies using macro- and micro-rheology techniques. Our measurements reveal the differences between the mechanical properties of gels and glasses.

The glassy samples are homogenous on all length scales probed in our experiments ( $l > 0.5 \mu\text{m}$ ). This is further confirmed by comparing microrheology and conventional macrorheology results. We find that measurements at different scales all give the same results. Thus, there is no evidence for spatial inhomogeneity as expected for glassy systems in general.

In the gels, however, along with the evolution from a liquid-like state to a viscoelastic state, inhomogeneities develop in time. These inhomogeneities are detected by measuring the local shear moduli at different positions within the samples at nearly equal waiting times.

Another difference between gels and glasses that we observed is that the change in the ratio  $G'/G''$  is much more rapid for a gel than for a glass as the material evolves from a purely viscous liquid to solid-like system.

When we track the values of the elastic modulus at a fixed frequency (here 0.05 Hz) at late stages of aging, when there is a crossover from a fast aging rate to a slower aging rate, we find that the elastic modulus scales

linearly with concentration. One can roughly estimate the plateau value for glasses as  $G'_P \propto kT/D^3$ , where  $D$  is the characteristic structural length of the system. We have taken  $D$  as half of the interparticle distance. This estimate predicts the order of magnitude fairly well. As shown in Fig. 13, the extrapolation of our data suggests that no glassy samples exist at concentrations lower than 1.6 wt%.

Therefore the elasticity for samples with lower concentrations should stem from a different mechanism. Indeed, in such samples the aging proceeds through gel formation. For comparison, we have shown the elastic modulus of a gel sample of 0.8 wt%, 6mM in Fig. 13.

Despite the differences between gels and glasses, we find a similar frequency dependence of the visco-elastic moduli for gels and glasses. The local viscoelastic moduli for both gels and glasses cross over from a single power law to the sum of two power laws around a certain time  $t_0$ . These results demonstrate the existence of two distinct contributions in the viscoelasticity of the system in the later stages of aging. In addition to a strongly frequency-dependent viscoelastic shear modulus at high frequencies  $\cong \omega^{0.7}$ , we also observe the slow development of a more elastic (only weakly frequency-dependent) shear modulus during the aging. The exponents of the

power laws follow exactly the same time course of evolution for different concentrations if we scale the aging time as  $t'_a = (t_w - t_0)/t_0$ . This result is independent of the sample being a gel or a glass.

The crossover from a single frequency-dependent component to a superposition of a strongly frequency-dependent viscoelastic component plus a weakly frequency dependent (elastic) component was previously interpreted in the context of polymer networks as being due to large inhomogeneities [29, 30]. Here the sum of two power-laws describes both gel (heterogeneous) and glass (homogeneous) local shear moduli, suggesting that locally the underlying physical process responsible for the evolution of gels and glasses is similar. This poses the rather puzzling question what the physical origin of the two power-laws in the viscoelasticity is.

**Acknowledgments** This research has been supported by the Foundation for Fundamental Research on Matter (FOM), which is financially supported by Netherlands Organization for Scientific Research (NWO). LPS de l'ENS is UMR8550 of the CNRS, associated with the universities Paris 6 and 7. C.F.S was further supported by the DFG Center for the Molecular Physiology of the Brain (CMPB).

- 
- [1] P. Sollich, F. Lequeux, P. Hebraud, M.E. Cates, Phys. Rev. Lett. **78**, 2020 (1997); S. M. Fielding and P. Sollich, M.E. Cates, J. Rheology **44**, 323 (2000); Soft and Fragile Matter: Nonequilibrium Dynamics, Metastability and Flow (Scottish Universities Summer School in Physics Proceedings) M.E. Cates.
- [2] P.N. Pusey and W. van Megen, Phys. Rev. Lett. **59**, 2083 (1987); W. van Megen, S. M. Underwood and P.N. Pusey *ibid.*, **67**, 1586 (1991); K. N. Pham, S. U. Egelhaaf, P. N. Pusey, W.C. K. Poon, Phys. Rev. **E69**, 011503 (2004).
- [3] M. Kroon, G.H. Wegdam, R. Sprik, Phys. Rev. **E54**, 6541 (1996).
- [4] D. Bonn, H. Kellay, H. Tanaka, G.H. Wegdam and J. Meunier, Langmuir **15**, 7534-7536 (1999), D. Bonn, H. Tanaka, H. Kellay, G.H. Wegdam and J. Meunier, Europhys. Lett. **45**, 52 (1998).
- [5] D. A. Weitz, J. S. Huang, M. Y. Lin and J. Sung, Phys. Rev. Lett. **54**, 1416(1985); M. Carpineti and M. Giglio, Phys. Rev. Lett. **68**, 3327 (1992); L. Cipelletti, S. Manley, R. C. Ball, and D. A. Weitz, Phys. Rev. Lett. **84**, 2275 (2000).
- [6] W. K. Kegel and A. van Blaaderen, Science **287**, 290 (2000).
- [7] K. N. Pham, G. Petekidis, D. Vlassopoulos, S. U. Egelhaaf, P. N. Pusey and W. C. K. Poon, Europhys. Lett. **75** (4), 624 (2006)
- [8] P. Levitz, E. Lecolier, A. Mourchid, A. Delville, and S. Lyonnard, Europhys. Lett. **49**, 672 (2000).
- [9] B. Ruzicka, L. Zulian and G. Ruocco, Phys. Rev. Lett. **93**, 258301 (2004); Langmuir **22** 1106 (2006)
- [10] D. Bonn, P. Coussot, H.T. Huynh, F. Bertrand and G. Debregeas, Europhys. Lett. **59**, 786 (2002).
- [11] M. Bellour, A. Knaebel, J.L. Harden, F. Lequeux and J.-P. Munch, Phys. Rev. **E67**, 031405 (2003), S. Kaloun, R. Skouri, M. Skouri, J. P. Munch and F. Schosseler Phys. Rev. **E72**, 011403 (2005).
- [12] S. Jabbari-Farouji, G. H. Wegdam, D. Bonn, Phys. Rev. Lett. **99**, 065701 (2007) [cond-mat/0611546].
- [13] T. Nicolai and S. Cocard, Langmuir **16**, 8189 (2000).
- [14] A gift from Van't Hoff Laboratory, Utrecht University
- [15] M. Atakhorrami, K.M. Addas and C. Schmidt; submitted to Rev. Scien. Inst.
- [16] M. Atakhorrami, PhD thesis, Vrije Universiteit Amsterdam 2006.
- [17] F. Gittes and C. F. Schmidt, Methods In Cell Biology, Vol. 55, p. 129 (1998).
- [18] F.C. MacKintosh and C.F. Schmidt, Current Opinion in Colloid & Interface Science **4**: 30 (1999).
- [19] S. Jabbari-Farouji, D. Mizuno, M. Atakhorrami, F.C. MacKintosh, C.F. Schmidt, E. Eiser, G.H. Wegdam and Daniel Bonn, Phys. Rev. Lett. **98**, 108302 (2007)[cond-mat/0511311].
- [20] T.G. Mason, and D.A. Weitz, Phys. Rev. Lett. **74**, 1250 (1995). T.G. Mason, H. Gang and D.A. Weitz J. Opt. Soc. Amer. A **14**, 139 (1997).
- [21] F. Gittes, B. Schnurr, B. P.D. Olmsted, F.C. MacKintosh, and C.F. Schmidt, Phys. Rev. Lett. **79**, 3286 (1997); B. Schnurr, F. Gittes, F.C. MacKintosh, C.F. Schmidt, Macromolecules **30**, 7781 (1997).
- [22] M. Buchanan, M. Atakhorrami, J.F. Paliarne, F.C. MacKintosh and C.F. Schmidt, Phys. Rev. **E72**, 011504 (2005); M. Atakhorrami and C.F. Schmidt, Rheologica Acta **45**(4) 449 (2006).
- [23] K. M. Addas, C. F. Schmidt and J. X Tang, Phys. Rev.

- E70**, 021503 (2004)
- [24] M. Atakhorrami, J. Sulkowska, K. M. Addas, G. H. Koenderink, A. Levine, F. MacKintosh, and C.F. Schmidt, Phys. Rev. **E73**, 061501 (2006).
- [25] A.J. Levine and T.C. Lubensky, Phys. Rev. **E65**, 011501 (2001).
- [26] S. Jabbari-Farouji, G. H. Wegdam, D. Bonn, in preparation.
- [27] S. Jabbari-Farouji, PhD thesis, University of Amsterdam
- 2007.
- [28] V. Trappe and D.A. Weitz, Phys. Rev. Lett. **85** 449 (2000).
- [29] M.L. Gardel, J.H. Shin, F.C. MacKintosh, L. Mahadevan, P.A. Matsudaira and D.A. Weitz, Phys. Rev. Lett. **93** 188102 (2004).
- [30] F. Brochard and P.G. de Gennes, Macromolecules **10** 1157 (1977); S.T. Milner, Phys. Rev. **E48** 3674 (1993).